



HAL
open science

A minimal model of self propelled locomotion

Jesús Sánchez-Rodríguez, Christophe Raufaste, Médéric Argentina

► **To cite this version:**

Jesús Sánchez-Rodríguez, Christophe Raufaste, Médéric Argentina. A minimal model of self propelled locomotion. *Journal of Fluids and Structures*, 2020, 97, pp.103071. 10.1016/j.jfluidstructs.2020.103071 . hal-02908041

HAL Id: hal-02908041

<https://hal.science/hal-02908041>

Submitted on 6 Feb 2022

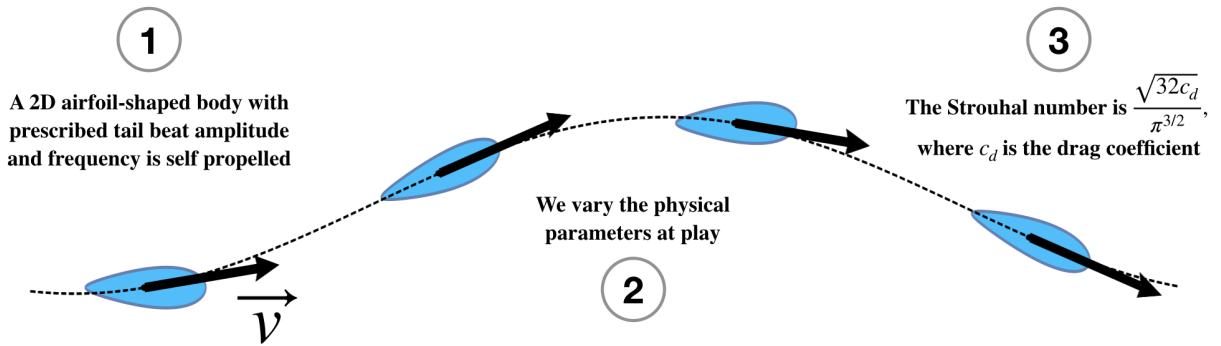
HAL is a multi-disciplinary open access archive for the deposit and dissemination of scientific research documents, whether they are published or not. The documents may come from teaching and research institutions in France or abroad, or from public or private research centers.

L'archive ouverte pluridisciplinaire **HAL**, est destinée au dépôt et à la diffusion de documents scientifiques de niveau recherche, publiés ou non, émanant des établissements d'enseignement et de recherche français ou étrangers, des laboratoires publics ou privés.

Graphical Abstract

A minimal model of self propelled locomotion

Jesús Sánchez-Rodríguez, Christophe Raufaste, Médéric Argentina



Highlights

A minimal model of self propelled locomotion

Jesús Sánchez-Rodríguez, Christophe Raufaste, Médéric Argentina

- Fish locomotion is studied with a two-dimensional thin airfoil-shaped body, which kinematics reduces to the tail beat amplitude and frequency, both in the transient and steady states
- Several parameters are studied both theoretically and with numerical simulations: length of the body, amplitude and frequency of the tail motion, dimensionless mass, position of the center of mass, and drag coefficient
- An analytical expression is found for the Strouhal number, which is strongly correlated to the drag coefficient while the other parameters can be neglected at the first-order approximation.

A minimal model of self propelled locomotion

Jesús Sánchez-Rodríguez^a, Christophe Raufaste^a and Médéric Argentina^a

^aUniversité Côte d'Azur, CNRS, Institut de Physique de Nice, 06100 Nice, France

ARTICLE INFO

Keywords:

fish locomotion
turbulent regime
Strouhal number
model
thrust
drag

ABSTRACT

Fish locomotion is a complicated problem in the context of fluid-structure interaction and it is still not understood what is linked to biology and what is linked to mechanics. Measurements performed on natural fish and artificial systems reveal that swimming at high Reynolds number is found in a narrow range of Strouhal numbers - a dimensionless combination of the swimming velocity, tail beat amplitude and frequency. With a minimal model of aquatic locomotion, we investigate how this number depends on the numerous parameters at play. We show a strong correlation with the drag coefficient, while the effect of the other parameters can be neglected at the first-order approximation.

1. Introduction

Fish across many species and scales cruise in a relatively narrow range of Strouhal numbers, around 0.3 (Triantafyllou, Triantafyllou and Gopalkrishnan (1991); Taylor, Nudds and Thomas (2003); Gazzola, Argentina and Mahadevan (2014); Saadat, Fish, Domel, Di Santo, Lauder and Haj-Hariri (2017)). This dimensionless parameter, $St = Af/U$, is a simple combination of the swimming velocity U , tail beat amplitude A and frequency f . The self propelled locomotion is usually modelled by accounting for the fluid-structure interaction and neglecting the biological aspects. In that sense, the constancy of the Strouhal number is found in the high Reynolds numbers - or turbulent - regime with typical Re larger than $10^3 - 10^4$. This indicates a correlation with the nature of the drag force, dominated by pressure drag over skin friction, and the possibility to derive a simple scaling argument to understand the almost constancy of the Strouhal number as a balance between thrust and drag per unit depth, which scale as $\rho f^2 A^2 L$ and $\rho U^2 L$ respectively with L the fish length (Gazzola et al. (2014)). In the same vein, numerous artificial systems have been studied in experiments and models such as flapping foils (Koochesfahani (1987); Triantafyllou, Triantafyllou and Grosenbaugh (1993); Schouveiler, Hover and Triantafyllou (2005)) or compliant robots (Gibouin, Raufaste, Bouret and Argentina (2018); Zhu, White, Wainwright, Di Santo, Lauder and Bart-Smith (2019)).

Some experiments consist in varying the kinematic parameters A and f and to find the free swimming velocity U . Experiments performed with flexible panels (Quinn, Lauder and Smits, 2014; Saadat et al., 2017) and robots (Gibouin et al., 2018) undergoing heaving or pitching motions show that St is relatively constant, independently of f , as long as the dimensionless amplitude A/L remains small. As an example it varies less than 50% up to $A/L = 0.35$ for the robotic fish studied by Gibouin et al. (2018), in agreement with the thrust-drag balance mentioned above. In addition Saadat et al. (2017) consider that an efficiency criterion holds at the same time, which leads to a maximal efficiency around $A/L \sim 0.2$, as observed in nature (Bainbridge, 1958; Hunter and Zweifel, 1971; Rohr and Fish, 2004; Saadat et al., 2017).

On the other hand, experiments performed with rigid foils undergoing heaving and pitching motions propose a slightly different approach: the Strouhal number is varied for a given value of A/L . For instance it varies in the range 0.1-1.5 for $A/L \sim 0.2$ in experiments by Quinn, Lauder and Smits (2015). The propulsive efficiency is called to set the value of parameters, here St , and in that case the efficiency exhibits a maximum in the range 0.2-0.4 (Floryan, Van Buren and Smits (2018)).

While both a thrust-drag balance and an efficiency criteria are called at the same time with these different kind of systems, they set the values of A/L and St in different ways. It is still remarkable that these values are consistent with data obtained with natural fish in all cases. While the thrust-drag balance sets the order of magnitude of St (Gazzola et al. (2014)), it is remarkably fixed for free-swimming flexible structures, while it needs to be fine-tuned with an efficiency criterion for rigid systems undergoing heaving and pitching motions.

*mederic.argentina@univ-cotedazur.fr (M. Argentina)
ORCID(s):

Here we consider a simple model of aquatic locomotion to give further insights. We consider an airfoil-shaped, rigid and two-dimensional body performing a kinematic motion of amplitude A and frequency f . This body is free to move contrary to the experiments and is not prescribed to a given position. Only the orientation of the body with respect to a fixed frame of reference is forced and the rest is predicted by the second law of Newton. Expressions of the thrust and drag forces are based from the Theodorsen approach (Theodorsen (1935); Garrick (1936)) in the realm of perfect fluid, but we take into account an additional pressure drag, which can not be predicted in this framework. First, we show that such a swimmer initially at rest, starts to propel itself as the body oscillates. It exhibits both heaving and pitching motions and will finally cruise at constant speed whatever the initial conditions. Second, in the limit of small tail beat amplitude, we predict the locomotion velocity, and the Strouhal number. The latter does not depend on the tail beat frequency but is strongly correlated with the drag coefficient. For classical values of this coefficient, we find that St is almost constant, around $0.1 - 0.3$, in agreement with natural and artificial systems. In addition to this very good predictive capacity, we demonstrate how the physical parameters prescribe the phase angle between pitch and heave.

The article is composed as follows. After having introduced the problem, we present our model (Sec. 2) and the methods (Sec. 3) to analyse it. Sec. 4 is devoted to present the results of our approaches, and the last section gathers some concluding remarks.

2. Model

We assume our swimmer to be a two-dimensional thin body, composed by a point mass (2D mass m , unit $\text{kg}\cdot\text{m}^{-1}$) attached to a straight, rigid and massless foil of length L , which models the tail. In the reference frame of the laboratory, this tail is inclined by an angle α with respect to the x axis and is counted positive clockwise, as seen in Fig. 1. The center of mass is located at the algebraic distance $aL/2$ from the center of the tail (with a a dimensionless number in the range $[-1, 1]$). As example, for $a = 0$, the center of mass coincides with the center of the tail. The swimmer evolves inside an inviscid fluid of density ρ . Swimming is triggered by imposing the harmonic forcing

$$\alpha(t) = \alpha_0 \sin(\omega t). \quad (1)$$

We expect the swimmer to evolve in average in the x direction, because the trailing edge sits in the right part of the foil. We note $u(t)$ and $v(t)$ respectively the instantaneous velocities of the center of mass in the x and y directions. In the following, we will define $U = \langle u(t) \rangle$ as the average swimming velocity in steady state, where $\langle \cdot \rangle$ consists in averaging over one period of the harmonic forcing α .

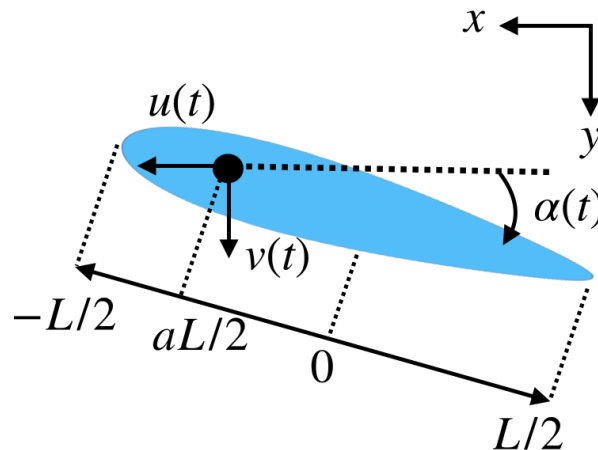


Figure 1: Sketch of the swimmer and relevant quantities. We note m the mass of the swimmer per unit length in the third dimension and ρ the density of the fluid. Angles are counted positively clockwise.

Assuming small angles ($\alpha_0 \ll 1$), we rely on the approach developed by Theodorsen (1935) and Garrick (1936) to calculate the forces at play. Since our swimmer is free to move, the position of the axis of rotation defined in

Theodorsen is not relevant here and everything can be expressed in terms of the position of the center of mass only. In Theodorsen's equations we can set the position of the center of mass at $aL/2$ by setting $x_\alpha = 0$ and $\dot{h} = v(t)$ with Theodorsen's notations. In addition, $\beta = 0$ since we do not consider any flap. The y direction force, F_y , writes:

$$F_y = -\pi\rho \left(\frac{L}{2}\right)^2 \left[u(t)\alpha'(t) + u'(t)\alpha(t) + v'(t) - a\frac{L}{2}\alpha''(t) \right] - 2\pi\rho \frac{L}{2}u(t)C(k) \left[u(t)\alpha(t) + v(t) + \left(\frac{1}{2} - a\right)\frac{L}{2}\alpha'(t) \right] + O(\alpha^3), \quad (2)$$

where $C(k = \omega L/u(t))$ is a function introduced by Theodorsen (1935) to account for the history of the shed vortices. Here two comments come into sight.

- First, $C(k)$ is difficult to compute because it is a non-local quantity that accounts for the vorticity distribution in the entire wake of the airfoil. Nevertheless, if we consider a treatment of the problem with complex periodic variables and set $\alpha = \alpha_0 e^{i\omega t}$, this function noted $C_{Th}(k)$ becomes complex and reduces to a composition of Hankel functions (Theodorsen (1935)). In the framework developed here, the argument $k \gtrsim 1$ and $C_{Th}(k)$ is well approximated by a real constant equal to 1/2 (Theodorsen (1935); Garrick (1936)), which means that we can set $C = 1/2$ as well in the treatment of the problem with real quantities. In the following, we treat the influence of the wake by setting $C = 1/2$.
- Second, the term $u'(t)\alpha(t)$ does not appear in Theodorsen's derivation but arises immediately as soon as we consider temporal variations of u , as remarked in Greenberg (1947). Theodorsen's approach exploits the linearity of the equation of the velocity potential, and predicts $F_y(t)$ by adding the potentials induced by the motions of the airfoil - like the vertical displacement and the variation of the attack angle. To take into account the effect of an unsteady streaming flow, it is necessary to add the supplementary potential induced by a longitudinal velocity $u(t)$, which turns out to be zero, because the airfoil is infinitely thin. Consequently the potential flow of an airfoil, submitted to an unsteady velocity $u(t)$ takes the same form as prescribed in Theodorsen's model. Nevertheless, to compute the pressure exerted by the fluid, we use, as usual, the Bernoulli relation which generates the extra term $\alpha(t)\dot{u}(t)$, as in Greenberg (1947).

Following Garrick (1936), the force induced by the inviscid fluid in the x direction, F_x accounts for two contributions: $F_x = \alpha F_y + F_{LE} + O(\alpha^4)$

1. The first contribution αF_y corresponds to the projection of the Theodorsen pressure in the x direction
2. F_{LE} stands for a force that results from the presence of a singular flow: an infinitely thin body would lead to a divergence of the pressure at the leading edge of the swimmer. To avoid for this non physical effect, we use the expression of Garrick (1936), by adding F_{LE} .

$$F_{LE} = \pi\rho \left(\frac{L}{2}\right) \frac{1}{\sqrt{2}} \left[2C \left(v(t) + u(t)\alpha(t) + \left(\frac{1}{2} - a\right)\frac{L}{2}\alpha'(t) \right) - \frac{L}{2}\alpha'(t) \right]^2 \quad (3)$$

We remark here that Garrick introduced a regularization to smooth the horizontal velocity, i.e. the horizontal component of the gradient of the velocity potential, and therefore does not introduce any temporal derivative of $u(t)$, $v(t)$ or $\alpha'(t)$. The resulting force, known as the leading edge suction, appears to be significant for biological swimmers, as shown by recent measurements (Lucas, Lauder and Tytell (2020)).

In this approach, note that F_y is a second-order approximation in α_0 , while F_x accounts for third-order terms as well. Finally, the velocities of the swimmer are calculated following the second law of Newton:

$$mu' = F_x - \rho c_d Lu(t)^2 \quad (4)$$

$$mv' = F_y \quad (5)$$

We recall here that these momentum balances are written per unit length. To take into account the drag induced by the boundary layers, we have added an horizontal pressure drag force. Defining the wetted perimeter as $2L$, this force writes $\frac{1}{2}\rho u(t)^2 c_d(2L)$, with the drag coefficient c_d .

3. Methods

First, the equations are transformed to use dimensionless quantities. Time and velocities are scaled by $1/\omega$ and $\omega L/2$ respectively. We define $\tilde{t} = \omega t$, $\tilde{u} = \frac{2u}{\omega L}$ and $\tilde{v} = \frac{2v}{\omega L}$. Using these quantities, we write the set of dimensionless equations summarized in the appendix A. We deduce four relevant dimensionless parameters: α_0 , c_d , a and

$$M = 4m/(\pi\rho L^2), \quad (6)$$

where M is the dimensionless mass of the swimmer. Given that we consider a thin swimmer, we expect $M \ll 1$. In regard of the dimensional analysis, any dimensionless calculated quantity will be a function of these four parameters. Such is the case of the dimensionless steady velocity \tilde{U} , of the ratio $A/L = \frac{1}{2}\tilde{A}$ of the tail beat amplitude (defined as the peak-to-peak amplitude) to the length or of the Strouhal number $St = Af/U = \frac{\tilde{A}}{2\pi\tilde{U}}$.

We study the set of dimensionless equations using direct simulations, and perturbative expansion. For both approaches, we take $\tilde{u}(0) = \tilde{v}(0) = 0$. We have checked with the numerical approach that these values do not change the behavior in the steady state.

3.1. Perturbative approach

To go in depth in understanding this minimal model and how the different parameters influence the swimming, we perform a perturbative development in order to determine an analytical expression for the velocities. The parameter which allows our perturbative expansion is α_0 , which is assumed to be small compared to the unity, because self propelled swimmers rarely exhibit high values for α . In fact, we show in Sec. 4.2 that $\alpha_0 \sim A/L$, which is equal to 0.2 for most fish as written in introduction.

We will rename α_0 as ε all along this section and $\alpha(t) = \varepsilon \sin(t)$. Thorough calculations are reported in the appendix B. Given the small angle hypothesis, the expressions of the velocities can be expanded to the second order in ε . In the limit $M \ll 1$, the velocities in the steady state write:

$$\tilde{u}(\tilde{t}) = \varepsilon \sqrt{\frac{\pi}{32c_d}} + \varepsilon^2 \left[\frac{1}{32M} \sin(2\tilde{t}) \right] + O(\varepsilon^3) \quad (7)$$

$$\tilde{v}(\tilde{t}) = \varepsilon a \cos(\tilde{t}) - \varepsilon^2 \frac{3}{2} \sqrt{\frac{\pi}{32c_d}} \sin(\tilde{t}) + O(\varepsilon^3) \quad (8)$$

$\tilde{u}(\tilde{t})$ and $\tilde{v}(\tilde{t})$ reach their steady state values after a transient time $\tilde{t} \sim M/\varepsilon\sqrt{c_d}$: this reflects that a heavy swimmer will need time to reach its cruising velocity. An oscillatory function, whose frequency is doubled as compared to the driving angle, is superposed to the mean swimming velocity. We remark here that this expansion in terms of the small parameter ε is formal and might break the assumption of a small transverse velocity in comparison to the longitudinal velocity. Nevertheless, on one hand, we recall that the pressure drag coefficient is quite small, of order 0.01 (see Sec. 4), and this value permits to finally verify that the locomotion velocity is larger than the transverse velocity. On the other hand, experimental data suggest that the thrust derived from the linear theory likely extends beyond the small amplitude regime (Mackowski and Williamson (2015); Fernandez-Feria and Sanmiguel-Rojas (2019)). The dimensionless swimming velocity $\tilde{U} = \langle \tilde{u}(\tilde{t}) \rangle$ is given by

$$\tilde{U} = \varepsilon \sqrt{\frac{\pi}{32c_d}} + O(\varepsilon^3). \quad (9)$$

The steady state transverse velocity $\tilde{v}(\tilde{t})$ is a harmonic function of time. By integrating this velocity, the dimensionless y -position of the center of mass is given by $\tilde{y}_c(\tilde{t}) = \varepsilon a \sin(\tilde{t}) + \varepsilon^2 \frac{3}{2} \sqrt{\frac{\pi}{32c_d}} \cos(\tilde{t}) = \sqrt{\varepsilon^2 a^2 + \varepsilon^4 \frac{9}{4} \frac{\pi}{32c_d}} \sin(\tilde{t} - \phi)$. From this expression we can infer the phase angle ϕ between the oscillations of the position of the mass center and the driving angle α .

$$\phi = \frac{-\pi}{2} + \arctan \left[\frac{8a}{3\varepsilon} \sqrt{\frac{2c_d}{\pi}} \right]. \quad (10)$$

Still in the small angle limit, the dimensionless y -position of the tip of the tail is given by $\tilde{y}_t = \tilde{y}_c + (1 - a)\alpha = \varepsilon \sin(\tilde{t}) + \varepsilon^2 \frac{3}{2} \sqrt{\frac{\pi}{32c_d}} \cos(\tilde{t})$. The dimensionless tail beat amplitude \tilde{A} is thus given by

$$\tilde{A} = 2\varepsilon \sqrt{1 + \left(\varepsilon \frac{3}{2} \sqrt{\frac{\pi}{32c_d}} \right)^2} + O(\varepsilon^3) = 2\varepsilon + O(\varepsilon^3). \quad (11)$$

As a consequence the tail beat amplitude A is given by $2\varepsilon L/2$ and $A/L = \alpha_0$. The position of the tail is in-phase with the driving angle, while the phase of the position of the center of mass depends on a : it is in-phase if $a \rightarrow 1$ and the phase shift equals $-\pi$ if $a \rightarrow -1$.

With the dimensionless quantities, the Strouhal number $St = Af/U$ writes $St = \frac{\tilde{A}}{2\pi\tilde{u}}$. Given that \tilde{u} and \tilde{A} are calculated up to the second order in ε , St can be calculated up to the first order in ε :

$$St = \frac{\sqrt{32c_d}}{\pi^{3/2}} + O(\varepsilon^2). \quad (12)$$

In this first-order approximation, only the constant term is nonzero. Remarkably, it emphasizes that the Strouhal number is strongly correlated to the drag coefficient and barely depends on the other parameters.

3.2. Numerical approach

The equations are solved numerically with a Runge-Kutta method, at the fourth-order approximation (Press, Teukolsky, Vetterling and Flannery (2007)). We impose as initial conditions $\tilde{u}(0) = \tilde{v}(0) = 0$, and let our model evolves towards the cruising locomotion regime, which is reached after the aforementioned transient time $M/\alpha_0\sqrt{c_d}$.

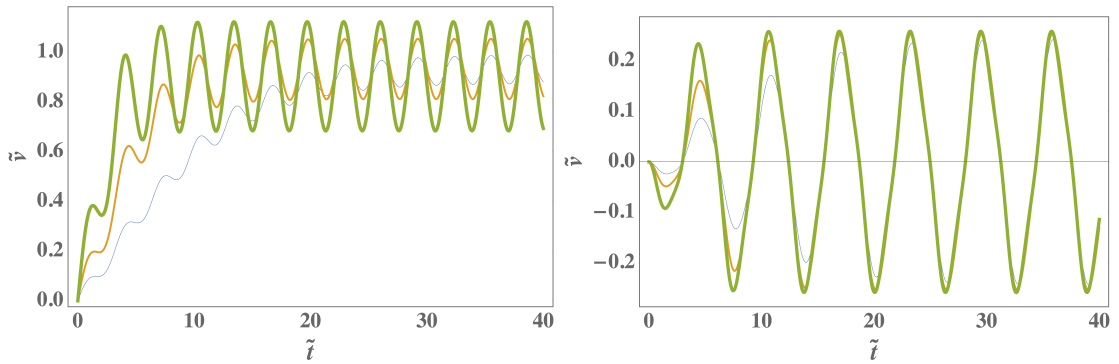


Figure 2: \tilde{u} and \tilde{v} as functions of \tilde{t} for the set of parameters [$\alpha_0 = 0.2$, $a = 0$, $c_d = 0.01$] and $M = 0.01, 0.02$ and 0.04 represented by the bold green, regular orange and thin blue lines respectively.

In all our simulations, the forcing in the pitch results in a cruising self propelled swimmer, for physically acceptable dimensionless parameters. In Fig. 2, we show a typical time evolution of the velocities \tilde{u} and \tilde{v} : as expected after a transient time which depends on M , the swimmer cruises in the steady state regime. Theodorsen's approach has been designed for a finite stream velocity. The model is robust with respect to the unsteadiness but is expected to be less precise in the transient regime, in particular if the swimmer starts from rest.

We remark here that the horizontal component of the locomotion oscillates around the steady value given by Eq. (9), with a frequency doubled with respect to the pitch forcing. We present in the Fig. 3 the dynamics of the angle α , the y -position of the center of mass \tilde{y}_c and the x -component of the velocity, obtained after the transient regime. $\tilde{u}(\tilde{t})$ oscillates twice faster than α and \tilde{y}_c , as predicted by the asymptotics, Eqs. (7,8). We will directly address the phase angle between pitch and heave in Sec. 4.3.

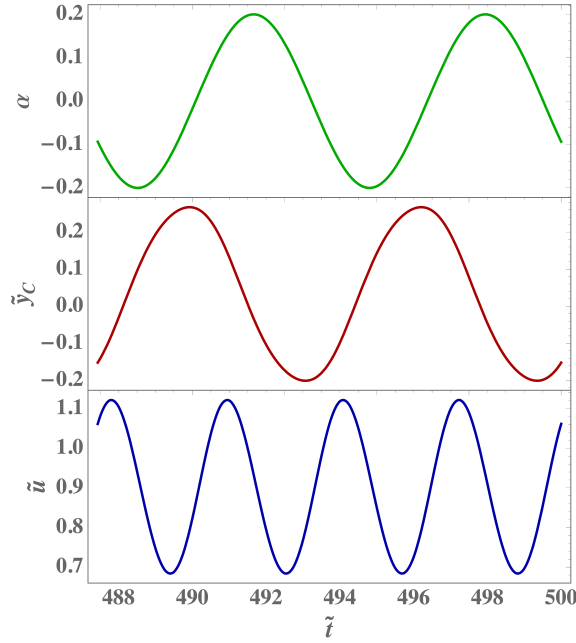


Figure 3: α , \tilde{y}_c and \tilde{u} as functions of \tilde{t} in the steady state for the set of parameters [$\alpha_0 = 0.2$, $a = 0$, $M = 0.01$, $c_d = 0.01$].

4. Results

The model depends on four dimensionless numbers and it is necessary to explore the parameter space in order to gain a complete outlook of the predictions of the system. In this part, we systematically study the effects of varying the values of α_0 , a , M and c_d . We then vary most of these parameters while maintaining some of them fixed. We tune our controlling parameters to the typical values measured in underwater swimming animals.

The reference values are set to [$\alpha_0 = 0.2$, $a = -1/2$, $M = 0.01$ and $c_d = 0.01$]. The perturbative analysis show that $\alpha_0 \simeq A/L$. Consequently, we have chosen as reference value $\alpha_0 = 0.2$, which is typical for fish (Bainbridge (1958); Hunter and Zweifel (1971); Rohr and Fish (2004); Saadat et al. (2017)). $a = -1/2$ corresponds to the particular case, where the center of mass is situated in the middle of the leading part of the fish. Since the swimmer is considered as a thin body, we expect $M \ll 1$. $M = 0.01$ is taken quite arbitrarily since we will show that in this limit, M does not have a significant effect on the measured quantities in the steady state. Values of the drag coefficient c_d are more difficult to infer from experiments since they require measurements when fish do not make any movement. Nevertheless some data were collected either with dead fish or during gliding deceleration. Lighthill reviewed data obtained with salmon, herring and trout and emphasized coefficients around 0.01 (Lighthill (1971)). Cods exhibit value around 0.011 – 0.015 (Videler (1981)), bluegill around 0.015 (Tandler, Gellman, De La Cruz and Ellerby (2019)) and dolphins between 0.003 and 0.03 (Lang (1975); Videler and Kamermans (1985)). The drag coefficient seems to depend on the experimental procedure, but in most cases the coefficients range between 0.01 and 0.1 for Reynolds numbers ranging between 10^3 and $3 \cdot 10^6$ (Tandler et al. (2019)). In the light of these measurements, we take $c_d = 0.01$ as the reference value.

In what follows, we discuss the effect of the four parameters on the Strouhal number St , the amplitude to length ratio A/L and the phase angle ϕ .

4.1. Strouhal number

The Strouhal number is assessed from the steady state values of \tilde{U} and \tilde{A} in simulation. In Fig. 4, color plots represent St as a function of c_d (from 10^{-3} to 10^{-1}) and another parameter among α_0 (from 0.003 to 0.3), a (from -1 to 1) and M (from 10^{-3} to 10^{-1}). This choice follows the observation that St is strongly correlated to c_d around the reference values, independently of the other parameters. This is consistent with the first-order approximation obtained theoretically (see Eq. (12)).

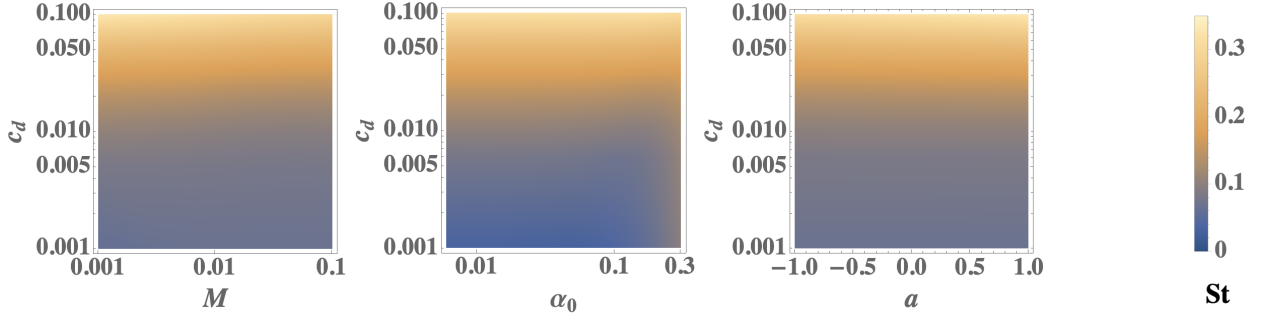


Figure 4: Variation of the Strouhal number, as the dimensionless numbers M , c_d , α and a are varied. From left to right: [$a = -1/2$ and $\alpha_0 = 0.2$], [$M = 0.01$ and $a = -1/2$] and [$M = 0.01$ and $\alpha_0 = 0.2$].

The perturbative approach and the numerical simulations are compared in Fig. 5. They are in very good agreement with each other and support the trend $St \propto \sqrt{c_d}$. More quantitatively, using the analytical expression of the Strouhal number at the first-order approximation, Eq. (12), with values of the drag coefficient measured with fish (0.01-0.1), we obtain values of St between 0.1 and 0.3. It is remarkable that our simple model recovers quantitatively the values measured in biological swimmers.

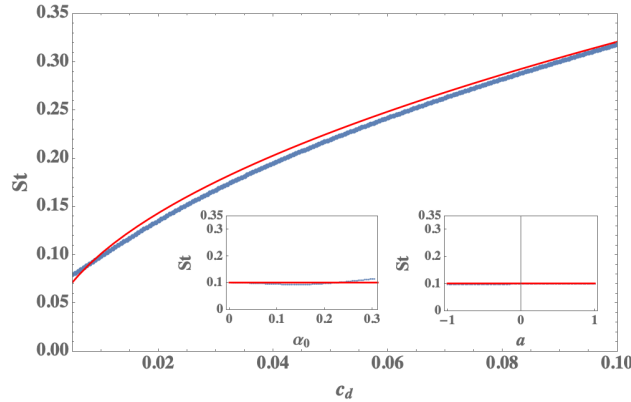


Figure 5: Strouhal number St as a function of the drag coefficient c_d [$\alpha_0 = 0.2$, $a = -1/2$ and $M = 0.01$]. The blue thick curve is obtained numerically, while the red curve corresponds to the prediction, Eq. (12). In the two insets, we display St as a function of α_0 [$a = -1/2$, $M = 0.01$ and $c_d = 0.01$] and a [$\alpha_0 = 0.2$, $M = 0.01$ and $c_d = 0.01$].

The study emphasizes that St barely vary with α_0 , a or M , but we recall that M and α_0 play a role in the transient state since the cruising swimming velocity \tilde{U} is reached after a typical time $\tilde{t} \sim M/\alpha_0 \sqrt{c_d}$ (Eq. (7) and Fig. 2). In the steady state where the swimmer has reached a nearly constant velocity, the inertia terms (closely related to the parameter M) become negligible and do not play any important role in the final swimming velocity, because this quantity is only determined by the equilibrium between thrust and drag forces as proved by Gazzola et al. (2014).

4.2. Tail beat amplitude

In Fig. 6, A/L is represented as a function of α_0 , both in simulations with the parameters [$a = -1/2$, $M = 0.01$ and $c_d = 0.01$] and in theory with the second-order approximation ($A/L = \tilde{A}/2$ in Eq. (11)). We see that $A/L \simeq \alpha_0$ is a very good approximation in the small angle limit. For $A/L = 0.2$ ($\alpha_0 = 0.17$), there is a 15% difference between what is obtained in simulation and in theory. This means that we probe the limit of the small angle regime (and the validity of our equations as well) and it is remarkable that natural fish are found there, at the onset of a strongly nonlinear regime where a third-order approximation would be required. Saadat et al. (2017) have shown that a criterion on the minimal energy assumption sets $A/L \sim 0.2$, which would emphasize that higher order terms become rapidly inefficient. The same argument would hold in the study performed by Floryan et al. (2018) since they find that the St

number at maximal efficiency is still very close to the one obtained in the small angle limit.

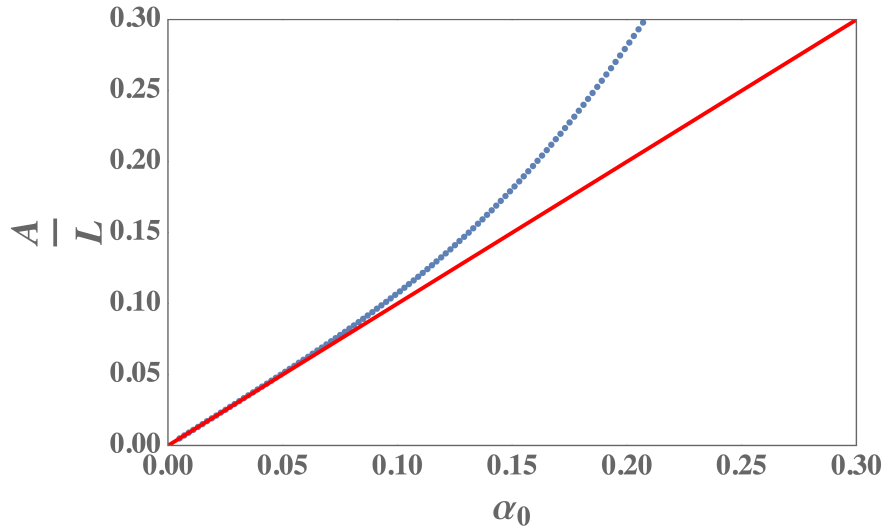


Figure 6: Tail beat amplitude A/L as a function of the driving angle α_0 . The blue symbols are obtained numerically, while the red curve corresponds to the prediction from Eq. (11).

4.3. Phase angle between heave and pitch

Our asymptotics computations conjecture through Eq. (10) the existence of a master curve for the phase ϕ as a function of $\frac{a\sqrt{c_d}}{a_0}$. We have collapsed various results of numerical computations onto this sigmoid curve in Fig. 7: it appears that our small angle approximation successfully predicts the phase angle between pitch and heave, and ϕ takes value in the ranges $[-\pi, -\pi/2]$ and $[-\pi/2, 0]$ for $a < 0$ and $a > 0$ respectively.

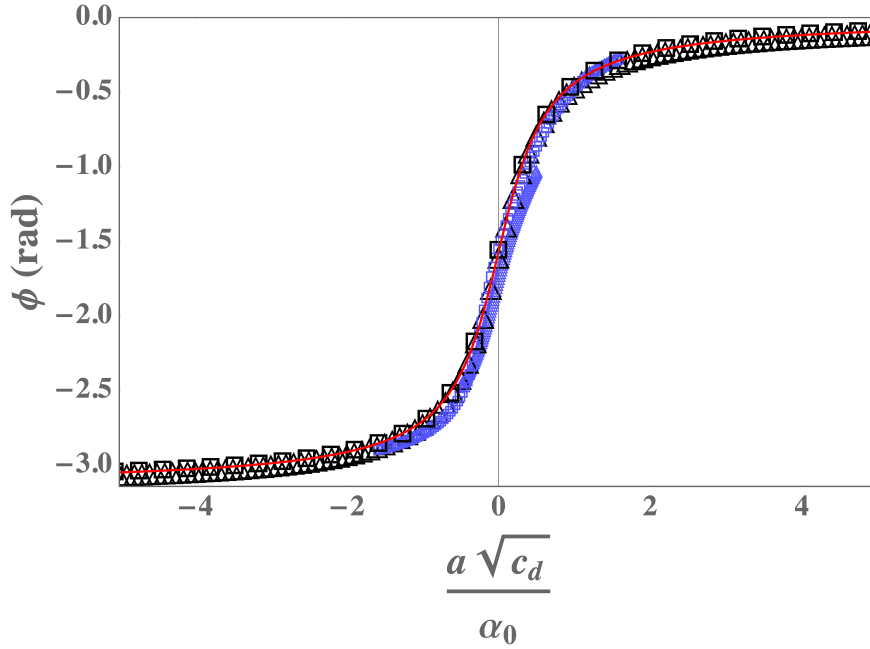


Figure 7: ϕ as a function of $\frac{a\sqrt{c_d}}{\alpha_0}$. The red curve is the analytical prediction of Eq. (10), $\phi(x) = -\pi/2 + \arctan\left(\frac{8}{3}\sqrt{\frac{2}{\pi}}x\right)$. In all the simulations we vary a and use the value $M = 0.01$, and the results are displayed for several values of c_d and α_0 . Triangles and squares correspond to $c_d = 0.01$ and 0.1 respectively, and large black and small blue symbols correspond to $\alpha_0 = 0.02$ and 0.2 respectively.

Thanks to pioneering studies in driving a NACA airfoil, there exist some measurements with respect to the synchronisation of the pitch and heave undulations (Anderson, Streitlien, Barrett and Triantafyllou (1998); Read, Hover and Triantafyllou (2003)). To compare our results with these studies, we define $\psi = \phi + \pi$ the phase angle between pitch and heave with angles α counted positively counterclockwise (all along our study we have used the clockwise definition taken by Theodorsen (1935)). The aforementioned studies demonstrate that the best thrust performance is reached as the phase angle ψ is close to 90° for a driven airfoil, or equivalently ϕ close to -90° , following our notation. In the light of our results, this suggests that the best thrust performance is obtained as $a\sqrt{c_d}/\alpha_0 \rightarrow 0$ or $|a| \ll \alpha_0/\sqrt{c_d}$.

We remark here that if $a < 0$, ψ tends to 0, for very low amplitude of the tail $\alpha_0 \rightarrow 0$. We also emphasize that the phase ψ is equal to 90° , independently of any controlling parameter if $a = 0$. All these arguments indicates that the location of the mass center should have an impact on the thrust performance.

5. Discussion

First, with our set of equations we expect St to be a function of the dimensionless quantities α_0 , c_d , a and M . None of them is a function of the tail beat frequency f . This means that the Strouhal number of a free-swimming, airfoil-shaped, rigid body does not depend on the frequency. This behavior is different from the one of the same kind of bodies performing pitching and heaving motions in classical water tunnel experiments (Quinn et al. (2015); Floryan, Van Buren, Rowley and Smits (2017)). In this case, the body is not free to move since the longitudinal position is fixed and the transverse motion is imposed. These constraints allow pitching and heaving motions to be set independently, which is accounted for by an additional dimensionless number that includes the tail beat frequency. With a free-swimming body, pitching and heaving motions can not be dissociated and the tail beat frequency is not relevant in determining the Strouhal number.

Second, the model makes explicit the trend $St \propto \sqrt{c_d}$ expected from a simple thrust-drag balance (Gazzola et al. (2014); Gibouin et al. (2018)). This result obtained with a free-swimming body in the small amplitude regime stems from a thrust scaling as $A^2 f^2$. This scaling seems to be validated beyond the small amplitude regime with constrained systems such as heaving foils (Quinn et al. (2014)), pitching foils (Floryan et al. (2017)), foils combining both of them

(Floryan et al. (2018)) and flexible robotic fish Gibouin et al. (2018).

6. Conclusions

We have studied a minimal model of fish locomotion. Our model is a 2D thin airfoil-shaped body which performs an oscillating motion; its cruising swimming velocity is predicted both numerically and theoretically in the small amplitude regime as a function of several parameters: the body length, the amplitude and frequency of the tail motion, the dimensionless mass, the position of the center of mass and the drag coefficient. We show that the Strouhal number is strongly correlated to the drag coefficient, while the effect of the other parameters can be neglected at the first order approximation. Given that natural fish exhibit values of c_d about 0.01-0.1, we find an almost constant Strouhal number, around 0.1-0.3, in very good agreement with values measured in biological swimmers. In addition, we uncover that the position of the center of mass has an effect on the phase angle between pitch and heave, and should consequently influence the thrust performance.

Our simple model accurately predicts the cruising motion of swimmers, but it remains dependent on the choice of the tail dynamics. It would be engaging to implement a mechanism that automatically selects the kinetics of the tail, without imposing either the amplitude α_0 or the beat frequency. We believe that a proprioceptive approach, like those proposed in Gazzola, Argentina and Mahadevan (2015), would be a good research direction.

Acknowledgements The authors acknowledge project funding by the UCA^{JEDI} IDEX grant (ANR-15-IDEX-01).

A. Appendix: Dimensionless equations

In this appendix we derive the dimensionless equations that we use in numerical simulations as well as in the perturbative treatment. Newton's second law with the forces calculated in Eqs. (2) and (3) plus pressure drag force reads:

$$mu' = F_x - \rho c_d Lu^2 \quad (13)$$

$$mv' = F_y \quad (14)$$

To obtain the dimensionless system we define the new dimensionless variables:

$$\tilde{u}(t) = \frac{2u(t)}{L\omega} \quad (15)$$

$$\tilde{v}(t) = \frac{2v(t)}{L\omega} \quad (16)$$

$$\tilde{t} = \omega t \quad (17)$$

Using these variables, we obtain the two dimensionless differential equations that we use for both the numerical and perturbative resolutions of our system.

$$M\tilde{u}'(\tilde{t}) = \tilde{F}_x - \frac{2}{\pi}c_d\tilde{u}^2(\tilde{t}) \quad (18)$$

$$M\tilde{v}'(\tilde{t}) = \tilde{F}_y \quad (19)$$

$$\tilde{F}_x = \alpha(\tilde{t})\tilde{F}_y + \frac{1}{\sqrt{2}} \left[2C \left(\frac{1}{\tilde{u}(\tilde{t})} \right) \left(\tilde{v}(\tilde{t}) + \tilde{u}(\tilde{t})\alpha(\tilde{t}) + \left(\frac{1}{2} - a \right) \alpha'(\tilde{t}) \right) - \alpha'(\tilde{t}) \right]^2 \quad (20)$$

$$\tilde{F}_y = - \left[\tilde{u}(\tilde{t})\alpha'(\tilde{t}) + \tilde{u}'(\tilde{t})\alpha(\tilde{t}) + \tilde{v}'(\tilde{t}) - a\alpha''(\tilde{t}) \right] - 2\tilde{u}(\tilde{t})C \left(\frac{1}{\tilde{u}(\tilde{t})} \right) \left[\tilde{u}(\tilde{t})\alpha(\tilde{t}) + \tilde{v}(\tilde{t}) + \left(\frac{1}{2} - a \right) \alpha'(\tilde{t}) \right], \quad (21)$$

Three dimensionless parameters appear: i) $M = 4m/(\pi\rho L^2)$ stands for the ratio of the swimmer mass to the added mass, ii) the drag coefficient c_d , iii) the dimensionless position of the center of mass a . The driving amplitude α_0 is the fourth relevant dimensionless parameter in the system. We recall that the influence of the shed vortices is measured by the function $C(1/\tilde{u}(\tilde{t}))$, which is set to $1/2$ because $1/\tilde{u}(\tilde{t}) \gtrsim 1$.

B. Appendix: Asymptotic approach

In this appendix, we derive the expression of the swimmer velocities as functions of all the dimensionless parameters. For simplicity (and only in this appendix), we remove the tilde above the dimensionless quantities. We assume that the driving amplitude is a small quantity, $\alpha_0 \ll 1$, and we use the notation $\varepsilon = \alpha_0$ to emphasize this hypothesis.

The angle $\alpha(t)$ writes as:

$$\alpha(t) = \frac{\varepsilon}{2i}e^{it} + c.c.,$$

where i is the imaginary unit, and $c.c.$ means complex conjugate. We use as an ansatz the following form of expansion:

$$u(t) = \varepsilon u_1(\tau) + \varepsilon^2 u_2(t) + \varepsilon^3 u_3(t) + O(\varepsilon^4) \quad (22)$$

$$v(t) = \varepsilon v_1(t) + \varepsilon^2 v_2(t) + O(\varepsilon^3), \quad (23)$$

where τ is used to identify a slow time scale $\tau = \varepsilon t$, to capture transient regimes. We have assumed that the first order of the horizontal velocity only depends on the slow time scale. The purpose of this appendix is to compute the leading orders of these expansions.

B.1. First Order

At order ε , we thoroughly determine the equation for the leading term of the transverse velocity:

$$v_1'(t) = \frac{a}{2(1+M)} (ie^{it} + c.c.).$$

This system is integrated into:

$$v_1(t) = \frac{a}{2(1+M)} (e^{it} + c.c.) + K_{v,1}, \quad (24)$$

where $K_{v,1}$ is an integration constant, that should be set to zero, to remove any vertical drift induced by the initial condition.

B.2. Second Order

At order ε^2 , we find the equation needed to determine the values of $u_1(\tau)$ and $u_2(t)$:

$$\begin{aligned} \frac{du_2(t)}{dt} = & -\frac{du_1(\tau)}{d\tau} - \frac{2c_d}{\pi M} u_1^2(\tau) + \frac{1}{2M} v_1^2(t) + \frac{1+M+4a(1+a+(a-1)M)}{16M(1+M)} \\ & - \frac{1+2a}{4M} v_1(t)e^{it} + \frac{1+M+4a(1+a+M(3+a))}{32M(1+M)} e^{2it} + c.c \end{aligned}$$

Given that $v_1(t) \propto \exp(it)$, we re-interpret this ODE under the following form

$$\frac{du_2(t)}{dt} = C + De^{2it} + c.c.$$

This system does not present harmonic terms because the forcing is a quadratic function of α in the horizontal velocity component. In this ODE, we remark that if C is not equal to zero, then the amplitude of $u_2(t)$ will increase linearly in time, such that at we will have $u_2 \gg u_1$ for large times, which breaks our expansion. To maintain the validity of the ansatz, we set $C = 0$ as a solvability condition. In other words, we invoke the Fredholm Alternative (Guckenheimer and Holmes (2002)), this restriction imposes an equation for $u_1(\tau)$:

$$\frac{du_1(\tau)}{d\tau} = -\frac{2c_d}{M\pi} u_1^2(\tau) + \frac{(1+M-2aM)^2}{16M(1+M)^2}$$

The initial condition to solve this equation is $u_1(0) = 0$,

$$u_1(\tau) = U_1 \tanh\left(\frac{\tau}{\tau_{sat}}\right), \quad U_1 = \frac{1+M-2aM}{4(1+M)\sqrt{c_d}} \sqrt{\frac{\pi}{2}}, \quad \tau_{sat}^{-1} = \frac{1+M-2aM}{2M(1+M)\sqrt{2\pi}} \sqrt{c_d}. \quad (25)$$

Hence $U = \varepsilon U_1$ is the asymptotic locomotion velocity, and τ_{sat} is defined as the characteristic transient time. In the limit for which M tends to zero, we obtain the simplified expression of the dominant term in $\tilde{u}(\vec{r})$ in Eq. (7)

Inserting the expression of $u_1(\tau)$ in the equation for $u_2'(t)$, we deduce the equation determining $u_2(t)$:

$$\frac{du_2(t)}{dt} = \frac{1+2M(1+6a)+M^2(1+4a(a+3))}{32M(1+M)^2} e^{2it} + c.c$$

We obtain by integrating:

$$u_2(t) = K_{u,1} - i \frac{1+2M(1+6a)+M^2(1+4a(a+3))}{64M(1+M)^2} e^{2it} + c.c \quad (26)$$

The equation $v_2(t)$ is deduced from the second order of the vertical momentum balance:

$$v_2'(t) = \frac{2a-3}{4(1+M)} u_1(\tau) - \frac{u_1(\tau)}{1+M} v_1(t),$$

and we solve it :

$$v_2(t) = K_{v,2} + i \frac{3+(3-2a)M}{4(1+M)^2} u_1(\tau) e^{it} + c.c. \quad (27)$$

Again the integration constant $K_{v,2}$ is set to zero to remove any vertical drift.

B.3. Third order

At this order, the expression becomes very lengthy, but the equation for u_3 presents the same form as those of u_2 :

$$u_3'(t) = C + \text{oscillating terms}$$

By invoking the solvability condition to maintain the validity of the expansion, the constant C is set to zero and we finally get:

$$K_{u,1} = 0$$

B.4. Phase shifting

To compute the phase angle between pitch and heave in the steady state, we first rewrite the expression of the lateral velocity at the second-order:

$$v(t) = \varepsilon \frac{a}{1+M} \cos(t) + \varepsilon^2 U_1 \frac{M(2a-3)-3}{2(1+M)^2} \sin(t),$$

using the results from Eqs. (24,27). In order to compare the heave and the pitch, we decompose this expression using only one trigonometric function:

$$v(t) = -\frac{a\varepsilon}{1+M} \sqrt{1 + \varepsilon^2 \left(U_1 \frac{M(2a-3)-3}{2a(1+M)} \right)^2} \sin(t - \phi_v)$$

$$\phi_v = \arctan \left[\frac{2a(1+M)}{\varepsilon U_1 (3 - M(2a-3))} \right],$$

which integrated gives the position of the tail:

$$y_t(t) = \frac{a\varepsilon}{1+M} \sqrt{1 + \varepsilon^2 \left(U_1 \frac{M(2a-3)-3}{2a(1+M)} \right)^2} \cos(t - \phi_v)$$

By comparing the above expression of $y_t(t)$ with respect to $\alpha(t) = \varepsilon \cos(t - \pi/2)$, we finally deduce the phase shifting in the heave-pitch motion:

$$\phi = -\frac{\pi}{2} + \phi_v = -\frac{\pi}{2} + \arctan \left[\frac{2a(1+M)}{\varepsilon U_1 (3 - M(2a-3))} \right]. \quad (28)$$

In the main text, we introduce this phase in the limit $M \rightarrow 0$, in the Eq. (10)

References

- Anderson, J., Streitlien, K., Barrett, D., Triantafyllou, M., 1998. Oscillating foils of high propulsive efficiency. *Journal of Fluid Mechanics* 360, 41–72.
- Bainbridge, R., 1958. The speed of swimming of fish as related to size and to the frequency and amplitude of the tail beat. *Journal of Experimental Biology* 35, 109–133. URL: <http://jeb.biologists.org/content/35/1/109>.
- Fernandez-Feria, R., Sanmiguel-Rojas, E., 2019. Comparison of aerodynamic models for two-dimensional pitching foils with experimental data. *Physics of Fluids* 31, 057104. doi:10.1063/1.5096337.
- Floryan, D., Van Buren, T., Rowley, C.W., Smits, A.J., 2017. Scaling the propulsive performance of heaving and pitching foils. *Journal of Fluid Mechanics* 822, 386–397. doi:10.1017/jfm.2017.302.
- Floryan, D., Van Buren, T., Smits, A.J., 2018. Efficient cruising for swimming and flying animals is dictated by fluid drag. *Proceedings of the National Academy of Sciences* 115, 8116–8118.
- Garrick, I.E., 1936. Propulsion of a flapping and oscillating airfoil. Report 567, National Advisory Committee for Aeronautics, Washington DC.
- Gazzola, M., Argentina, M., Mahadevan, L., 2014. Scaling macroscopic aquatic locomotion. *Nature Physics* 10, 758.
- Gazzola, M., Argentina, M., Mahadevan, L., 2015. Gait and speed selection in slender inertial swimmers. *Proceedings of the National Academy of Sciences* 112, 3874–3879. URL: <http://www.pnas.org/content/112/13/3874.abstract>, doi:10.1073/pnas.1419335112, arXiv:<http://www.pnas.org/content/112/13/3874.full.pdf>.
- Gibouin, F., Raufaste, C., Bouret, Y., Argentina, M., 2018. Study of the thrust–drag balance with a swimming robotic fish. *Physics of Fluids* 30, 091901. doi:10.1063/1.5043137.

- Greenberg, J.M., 1947. Airfoil in sinusoidal motion in a pulsating stream. Technical note 1326, National Advisory Committee for Aeronautics, Washington DC .
- Guckenheimer, J., Holmes, P., 2002. Nonlinear Oscillations, Dynamical Systems, and Bifurcations of Vector Fields. Applied Mathematical Sciences, Springer New York.
- Hunter, J.R., Zweifel, J.R., 1971. Swimming speed, tail beat frequency, tail beat amplitude, and size in Jack mackerel, *Trachurus symmetricus*, and other fishes. *Fishery Bulletin* 69, 253–266.
- Koochesfahani, M., 1987. Vortical patterns in the wake of an oscillating airfoil, in: 25th AIAA Aerospace Sciences Meeting.
- Lang, T.G., 1975. Speed, Power, And Drag Measurements of Dolphins and Porpoises. Springer US, Boston, MA. pp. 553–572. URL: https://doi.org/10.1007/978-1-4757-1326-8_5, doi:10.1007/978-1-4757-1326-8_5.
- Lighthill, M.J., 1971. Large-Amplitude Elongated-Body Theory of Fish Locomotion. *Proceedings of the Royal Society of London. Series B, Biological Sciences* 179, 125–138. URL: <http://www.jstor.org/stable/76021>.
- Lucas, K.N., Lauder, G.V., Tytell, E.D., 2020. Airfoil-like mechanics generate thrust on the anterior body of swimming fishes. *Proceedings of the National Academy of Sciences* 117, 10585–10592. doi:10.1073/pnas.1919055117.
- Mackowski, A.W., Williamson, C.H.K., 2015. Direct measurement of thrust and efficiency of an airfoil undergoing pure pitching. *Journal of Fluid Mechanics* 765, 524–543. doi:10.1017/jfm.2014.748.
- Press, W.H., Teukolsky, S.A., Vetterling, W.T., Flannery, B.P., 2007. Numerical Recipes 3rd Edition: The Art of Scientific Computing. 3 ed., Cambridge University Press, USA.
- Quinn, D.B., Lauder, G.V., Smits, A.J., 2014. Scaling the propulsive performance of heaving flexible panels. *Journal of Fluid Mechanics* 738, 250–267.
- Quinn, D.B., Lauder, G.V., Smits, A.J., 2015. Maximizing the efficiency of a flexible propulsor using experimental optimization. *Journal of Fluid Mechanics* 767, 430–448. doi:10.1017/jfm.2015.35.
- Read, D.A., Hover, F., Triantafyllou, M., 2003. Forces on oscillating foils for propulsion and maneuvering. *Journal of Fluids and Structures* 17, 163–183.
- Rohr, J.J., Fish, F.E., 2004. Strouhal numbers and optimization of swimming by odontocete cetaceans. *Journal of Experimental Biology* 207, 1633–1642. URL: <http://jeb.biologists.org/content/207/10/1633>, doi:10.1242/jeb.00948.
- Saadat, M., Fish, F., Domel, A., Di Santo, V., Lauder, G., Haj-Hariri, H., 2017. On the rules for aquatic locomotion. *Physical Review Fluids* 2, 083102.
- Schouveiler, L., Hover, F., Triantafyllou, M., 2005. Performance of flapping foil propulsion. *Journal of Fluids and Structures* 20, 949–959.
- Tandler, T., Gellman, E., De La Cruz, D., Ellerby, D.J., 2019. Drag coefficient estimates from coasting bluegill sunfish *Lepomis macrochirus*. *Journal of Fish Biology* 94, 532–534. URL: <https://onlinelibrary.wiley.com/doi/abs/10.1111/jfb.13906>, doi:10.1111/jfb.13906.
- Taylor, G.K., Nudds, R.L., Thomas, A.L., 2003. Flying and swimming animals cruise at a Strouhal number tuned for high power efficiency. *Nature* 425, 707–711.
- Theodorsen, T., 1935. General theory of aerodynamic instability and the mechanism of flutter. Report 496, National Advisory Committee for Aeronautics, Washington DC .
- Triantafyllou, G., Triantafyllou, M., Grosenbaugh, M., 1993. Optimal thrust development in oscillating foils with application to fish propulsion. *Journal of Fluids and Structures* 7, 205–224.
- Triantafyllou, M.S., Triantafyllou, G.S., Gopalkrishnan, R., 1991. Wake mechanics for thrust generation in oscillating foils. *Physics of Fluids A: Fluid Dynamics* 3, 2835–2837. URL: <https://aip.scitation.org/doi/10.1063/1.858173>, doi:10.1063/1.858173.
- Videler, J., 1981. Swimming movements, body structure and propulsion in cod *Gadus morhua*, pp. 1–27.
- Videler, J., Kamermans, P., 1985. Differences between upstroke and downstroke in swimming dolphins. *Journal of Experimental Biology* 119, 265–274. URL: <https://jeb.biologists.org/content/119/1/265>.
- Zhu, J., White, C., Wainwright, D.K., Di Santo, V., Lauder, G.V., Bart-Smith, H., 2019. Tuna robotics: A high-frequency experimental platform exploring the performance space of swimming fishes. *Science Robotics* 4. URL: <https://robotics.sciencemag.org/content/4/34/eaax4615>.